C. Brennen
J. C. Pearce
Division of Engineering and Applied Science, California Institute of Technology, Pasadena, Calif.

Granular Material Flow in Two-Dimensional Hoppers

1 Introduction

The flow and transport of granular media have been of major importance in commerce and industry for a long time; materials such as coal, ore, cement, grain, soap granules, sugar, sand, gravel, etc., flow in hoppers, bins, chutes, rotating drums, and moving bands. The desire to improve such transportation equipment and to reduce the energy expenditure has motivated interest in understanding the fluid mechanics of such bulk flows (Wieghardt [25][1]). Though transport, heat transfer, and other processes are often effected by fluidization we are concerned here with those situations in which the flow takes place with direct physical contact between the grains. Indeed the simplest situation is that in which the interstitial fluid (usually air) has a negligible effect on the equations of motion.

The purpose of this paper is to present a comparison of experimental data and analysis for the flow of dry granular media through a two-dimensional or wedge-shaped hopper. It will be seen that the analytical solution which begins with the constitutive postulates suggested by Jenike and Shield [9] of (*i*) intergrain Coulomb friction and (*ii*) isotropy produces results which are in good agreement with the experimental measurements.

2 Equations of Flow for a Cohesionless Granular Medium

The equations used to describe the flow of a granular medium (and by a flow we mean the process of continuous deformation which excludes quasi-flows in the form of undeforming plugs) are basically those of soil mechanics with inertial terms added. Here we confine ourselves to planar flow and u, v will initially denote the velocities in the directions of the Cartesian coordinates x and y. It is first assumed that the medium has reached a critical void ratio upon initiation of the continuous deformation and that the void ratio remains relatively constant thereafter; thus the medium is characterized by a constant bulk density, ρ (see Section 7) and continuity requires

$$\frac{\partial u}{\partial x} + \frac{\partial v}{\partial y} = 0. \tag{1}$$

This assumption is motivated by the observation of little global volumetric change during continuous deformation in simple uniform flows such as that involved in pure shearing (see Taylor [22], Jenike, Elsey, and Woolley [8], Jenike and Shield [9], Scott [18], Jenike [10]). However its validity is open to question in more complex flows; for example, the rupture zones observed by Templeton [23] seem at the very least to involve localized departures from the average bulk density.

The equations of motion which will be used neglect the effects of interstitial fluid and denote the integrain forces by a continuum stress tensor, σ:

$$\frac{\partial \sigma_{xx}}{\partial x} + \frac{\partial \sigma_{xy}}{\partial y} = \rho\left(\frac{\partial u}{\partial t} + u\frac{\partial u}{\partial x} + v\frac{\partial u}{\partial y}\right) \tag{2}$$

$$\frac{\partial \sigma_{yy}}{\partial y} + \frac{\partial \sigma_{xy}}{\partial x} - \rho g = \rho\left(\frac{\partial v}{\partial t} + u\frac{\partial v}{\partial x} + v\frac{\partial v}{\partial y}\right) \tag{3}$$

where the orientation of the coordinate system is such that the gravitational body force is in the negative y-direction.

It remains to discuss appropriate constitutive relations governing the continuous deformation of the granular medium and we shall adopt those suggested by the work of Drucker, Gibson, and Henkel [6], Shield [19] and Jenike and Shield [9]. It is first assumed that for the cohesionless materials considered here the maximum shear stress in the medium and the normal force on the corresponding principal plane are directly related by a simple Coulomb friction condition where the friction angle φ is assumed to be a constant material property. It follows that

$$\left[\left(\frac{\sigma_{xx} - \sigma_{yy}}{2}\right)^2 + \sigma_{xy}{}^2\right]^{1/2} \leq -\sin\varphi\left(\frac{\sigma_{xx} + \sigma_{yy}}{2}\right) \tag{4}$$

where the inequality is included merely to indicate the conditions prior to the initiation of flow or in regions of unyielded material which may exist in conjunction with flowing regions. Jenike and Shield [9] also indicate that the condition (4) may be readily modified to include the effects of cohesion, c, by addition of a term $-c\cos\varphi$ on the right-hand side; the effect could then be incorporated in an effective internal friction angle if one assumes that c is proportional to the mean stress ($\sigma_{xx} + \sigma_{yy}$). It should be noted that there have been other interpretations of the Coulomb condition (4) as a modification of a

[1] Numbers in brackets designate References at end of paper.

Contributed by the Applied Mechanics Division for publication in the JOURNAL OF APPLIED MECHANICS.

Discussion in this paper should be addressed to the Editorial Department, ASME, United Engineering Center, 345 East 47th Street, New York, N.Y. 10017, and will be accepted until June 1, 1978. Readers who need more time to prepare a Discussion should request an extension of the deadline from the Editorial Department. Manuscript received by ASME Applied Mechanics Division, November, 1976; final revision, July, 1977.

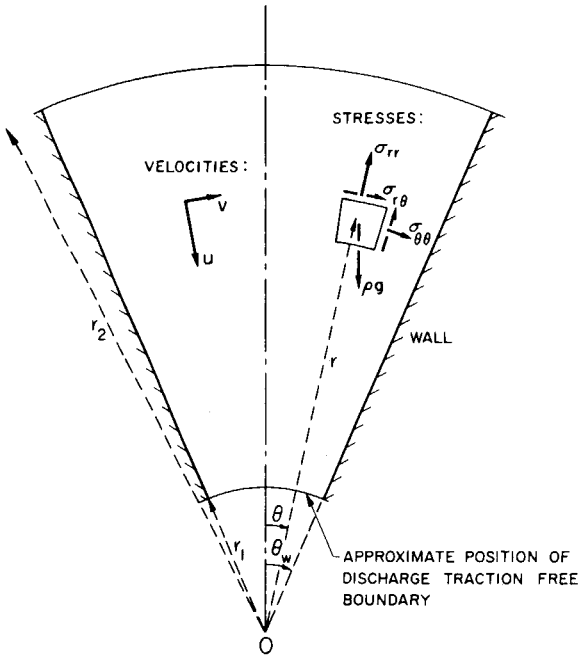

Fig. 1 Schematic and notation of two-dimensional hopper flow

Tresca or Von Mises yield criterion (Drucker [4, 5], Shield [19], Drucker, et al. [6]). Note also that unlike unconventional fluid mechanics these flows are dependent on the absolute magnitude of the mean stress.

The condition (4) is however insufficient in itself to complete the system of equations for the flow and stress fields; one other constitutive relation is necessary. We shall again follow Jenike and Shield [9] and others in adopting a condition of isotropy which states that the directions of principal stress and principal deformation coincide so that

$$\frac{\sigma_{xx} - \sigma_{yy}}{\sigma_{xy}} = \frac{2\left(\frac{\partial u}{\partial x} - \frac{\partial v}{\partial y}\right)}{\frac{\partial u}{\partial y} + \frac{\partial v}{\partial x}}. \tag{5}$$

It should however be mentioned that rigorous justification for either the condition of Coulomb friction or the condition of isotropy does not exist and both are open to question; recent experimental and theoretical investigations of these conditions have been reviewed by Mandl and Fernandez Luque [13]. For example, the observations of Drescher and de Josselin de Jong [2] and of Drescher [3] indicate that for relatively small deformations there are significant departures from isotropy due to the fact that deformation occurs by the propagation of nonisotropic dislocations.

From a simpler point of view, however, one might simply regard the conditions (4) and (5) as constitutive postulates whose practical value in predicting the flows of granular materials should be tested by comparison with measurements on simple rheological flows. But both of the rheological flows so widely used in fluid mechanics, namely, pipe flow and Couette flow, present difficulties in granular media because they may result in simple slippage at the solid walls and no continuous deformation of the granular medium unless the walls are very rough. Indeed hopper flows of the kind studied in this paper are among the simplest true flows and as such could be regarded as a rheological test of the constitutive postulates.

3 Flow in a Two-Dimensional Hopper

The primary purpose of this paper is to present a solution of the equations of the last section for the flow through a two-dimensional or wedge-shaped hopper of the kind shown in Fig. 1 and to compare the results with experimental measurement. For this purpose the governing equations (1)–(5) are rewritten in the polar coordinate system (r, θ) shown in Fig. 1 where for convenience u, v will now denote the velocities in the negative r, θ directions and the flow is assumed steady in time (see Section 9). Furthermore by defining Sokolovski [20] functions σ and γ such that

$$\begin{aligned} \sigma_{rr} &= -\sigma(1 - \sin\varphi\cos 2\gamma) \\ \sigma_{\theta\theta} &= -\sigma(1 + \sin\varphi\cos 2\gamma) \\ \sigma_{r\theta} &= \sigma(\sin\varphi\sin 2\gamma) \end{aligned} \tag{6}$$

the Coulomb friction condition (4) is automatically satisfied and the basic equations (1)–(3) and (5) become

Continuity

$$\frac{\partial u}{\partial r} + \frac{u}{r} + \frac{1}{r}\frac{\partial v}{\partial \theta} = 0 \tag{7}$$

r —Equation of Motion

$$\begin{aligned} (1 - \sin\varphi\cos 2\gamma)\frac{\partial \sigma}{\partial r} + 2\sigma\sin\varphi\sin 2\gamma\frac{\partial \gamma}{\partial r} - \sin\varphi\sin 2\gamma\frac{1}{r}\frac{\partial \sigma}{\partial \theta} \\ - \frac{2\sigma}{r}\sin\varphi\cos 2\gamma\left(1 + \frac{\partial \gamma}{\partial \theta}\right) \\ + \rho g\cos\theta = -\rho\left\{u\frac{\partial u}{\partial r} + \frac{v}{r}\frac{\partial u}{\partial \theta} - \frac{v^2}{r}\right\}. \end{aligned} \tag{8}$$

θ—Equation of Motion

$$\begin{aligned} (1 + \sin\varphi\cos 2\gamma)\frac{1}{r}\frac{\partial \sigma}{\partial \theta} - 2\frac{\sigma}{r}\sin\varphi\sin 2\gamma\left(1 + \frac{\partial \gamma}{\partial \theta}\right) \\ - \sin\varphi\sin 2\gamma\frac{\partial \sigma}{\partial r} \\ - 2\sigma\sin\varphi\cos 2\gamma\frac{\partial \gamma}{\partial r} - \rho g\sin\theta = -\rho\left\{u\frac{\partial v}{\partial r} + \frac{v}{r}\frac{\partial v}{\partial \theta} + \frac{uv}{r}\right\} \end{aligned} \tag{9}$$

Isotropy

$$2\frac{\partial u}{\partial r}\tan 2\gamma = \frac{\partial v}{\partial r} - \frac{v}{r} + \frac{1}{r}\frac{\partial u}{\partial \theta} \tag{10}$$

which must be solved for the unknown functions u, v, γ, and σ of r and θ.

A number of authors including Jenike [10], Pemberton [15], and Savage [16] have reported attempts to construct the flow and stress fields in a two-dimensional hopper. Jenike [10] begins with the assumption that the inertial terms on the right-hand sides of the equations of motion (8) and (9) are negligible. The immediate consequences of this is that the problem is reduced to one of static soil mechanics in which the velocities u and v and thus the discharge from the hopper is indeterminate. This can be readily demonstrated since following the omission of the inertial terms the remaining equations are homogeneous in the velocities which could therefore be multiplied by any arbitrary constant. Indeed it is the inertial terms which determine the flow velocities and the discharge. Nevertheless, Jenike's solution is of value in determining the kind of stress distribution one might expect in a hopper (see also Johanson [11]). Pemberton [15] has also reported inertia-less solutions similar to those of Jenike [10] but in which the isotropy condition was replaced by a somewhat modified version in which deformation occurs by shear along the characteristic curves of the stress equation. In the context of the present paper we should also note that neither of these inertialess solutions permit the existence of a "traction-free" surface ($\sigma = 0$) of the kind which must exist at discharge from the hopper.

Savage [16] (see also Sullivan [21]) on the other hand has reported a special solution in which the inertial terms are retained but in which the sidewalls are *frictionless* and gravity is assumed to act radially toward the point 0, Fig. 1, rather than vertically. Thus the problem is cylindrically symmetric with $v = 0$, $\gamma = 0$ and expressions for u, σ which are independent of θ. It is then a straightforward matter to show from the equation of continuity (7) that $u = A/r$ and from the equation of motion (8) that

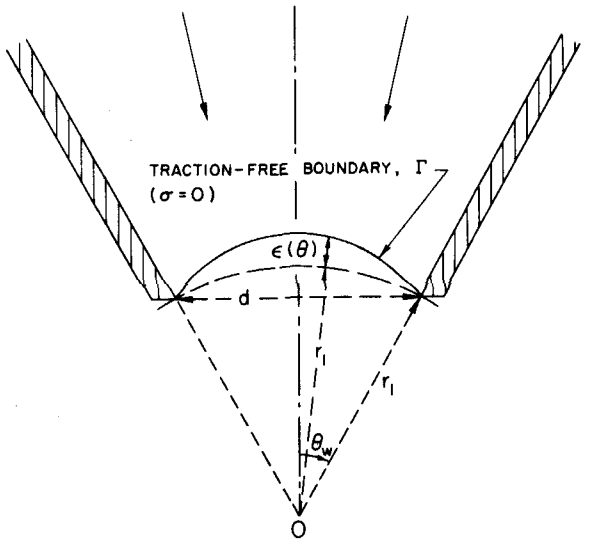

Fig. 2 Detail of the initially undetermined traction-free boundary, Γ, at discharge from the hopper

$$\sigma = Br^{\omega^*} + \frac{\rho g r}{(3\sin\varphi - 1)} - \frac{\rho A^2}{2r^2} \tag{11}$$

where A, B are constants and $\omega^* = 2\sin\varphi/(1-\sin\varphi)$ (a different expression for σ results in the special case $\sin\varphi = 1/3$). The conditions that $\sigma = 0$ at both upper ($r = r_2$) and lower ($r = r_1$) traction-free surfaces were then applied to determine the (uniform) velocity, U_D, at discharge:

$$\frac{U_D^2}{gr_1} = \frac{(\omega^*+2)}{(\omega^*-1)} \frac{\left[1 - \left(\frac{r_1}{r_2}\right)^{\omega^*-1}\right]}{\left[1 - \left(\frac{r_1}{r_2}\right)^{\omega^*+2}\right]}. \tag{12}$$

This expression yielded mass flow rates which were substantially greater than those exhibited in experiments. This motivated the present study in which friction on the walls is included and more plausible boundary conditions applied at the upper and lower surfaces. It will, however, be seen in the following section that the results for sidewalls with friction and with normal gravitational effects follow a similar form to the expression (12). Savage [16, 17] also reported an approximate solution of the flow-through a *conical* hopper which included inertia and wall friction; though the present solution for a two-dimensional hopper is superficially somewhat similar in form there are important differences. Savage's equations were the spherical coordinate version of those of the last section except that isotropy was not assumed. This was replaced by the assumption that the velocity u was independent of θ and that $v = 0$; thus isotropy was not satisfied. Furthermore the conditions at inlet to and discharge from the hopper which were adopted were those of traction-free surfaces ($\sigma = 0$) on $r = r_1$, r_2. We shall see that a more detailed examination of these boundaries leads to conditions which are better justified physically.

4 Analytical Solution for Flow in a Two-Dimensional Hopper

The purpose of this section is to present an approximate solution for the equations of motion (7)–(10) which includes the effects of friction between the granular media and the walls of a planar hopper (Figs. 1 and 2).

We first observe that specific values of γ at the walls $\theta = \pm\theta_w$ result from the assumption of Coulomb friction on the wall of the form

$$\left(\frac{\sigma_{r\theta}}{\sigma_{\theta\theta}}\right)_{\theta=\pm\theta_w} = \mp\tan\delta \tag{13}$$

where δ is the wall friction angle. From equations (6) this leads to the relation

$$(1 + \sin\varphi\cos 2\gamma_w)\tan\delta = \sin\varphi\sin 2\gamma_w \tag{14}$$

from which an exact value of $(\gamma)_{\theta=\theta_w} = (-\gamma)_{\theta=-\theta_w} = \gamma_w$ can be obtained numerically given only the two friction angles φ and δ. Thus assuming symmetry of the stress field about the center line $\theta = 0$, γ increases from zero at $\theta = 0$ to the known value of γ_w at $\theta = \theta_w$. (It should be noted in passing that the other choice of $\gamma = \pi/2$ on the center line with a corresponding change in the value on the wall can be shown to correspond to flow in the opposite direction to that of relevance here).

The present solution is constructed under the assumption that the opening angle, θ_w, is small though quantitative evaluation of the precise nature of this limitation which also involves the magnitude of the friction on the wall is delayed until later. We shall assume that both the flow and stress fields are symmetric about the center line, $\theta = 0$; in doing so it should be noted that nonsymmetric flows have been observed particularly by Lee, Cowin, and Templeton [12] but comment on this is delayed until Section 9. Thus the functions to be determined, namely, u, v, γ, and σ are expanded in the form

$$u = u_0(r) + u_2(r)\left(\frac{\theta}{\theta_w}\right)^2 + O\left(\frac{\theta^4}{\theta_w{}^4}\right) \tag{15}$$

$$v = v_1(r)\left(\frac{\theta}{\theta_w}\right) + v_3(r)\left(\frac{\theta}{\theta_w}\right)^3 + O\left(\frac{\theta^5}{\theta_w{}^5}\right) \tag{16}$$

$$\gamma = \gamma_1(r)\left(\frac{\theta}{\theta_w}\right) + \gamma_3(r)\left(\frac{\theta}{\theta_w}\right)^3 + O\left(\frac{\theta^5}{\theta_w{}^5}\right) \tag{17}$$

$$\sigma = \sigma_0(r) + \sigma_2(r)\left(\frac{\theta}{\theta_w}\right)^2 + O\left(\frac{\theta^4}{\theta_w{}^4}\right) \tag{18}$$

where, given a power series in θ, the indices are dictated by the symmetry of the field. The procedure is to expand the governing equations (7)–(10) in powers of θ and to obtain ordinary differential equations for u_0, v_1, γ_1, σ_0, etc., by equating coefficients of powers of θ. The hierarchy of equations which result begins with the θ^0 terms in the continuity equation (7) and the r equation of motion (8) which yield, respectively,

$$r\frac{\partial u_0}{\partial r} + u_0 + \frac{v_1}{\theta_w} = 0 \tag{19}$$

$$(1-\sin\varphi)r\frac{\partial\sigma_0}{\partial r} - 2\sigma_0\sin\varphi\left(1 + \frac{\gamma_1}{\theta_w}\right) + \rho g r = -\rho r u_0\frac{\partial u_0}{\partial r}. \tag{20}$$

Second, the θ^1 terms in the isotropy condition and the θ equation of motion produce

$$4\gamma_1 r\frac{\partial u_0}{\partial r} = \frac{2u_2}{\theta_w} + r\frac{\partial v_1}{\partial r} - v_1 \tag{21}$$

$$2r\sigma_0\sin\varphi\sigma_0\frac{\partial\gamma_1}{\partial r} - \frac{2}{\theta_w}(1+\sin\varphi)\sigma_2 + 4\gamma_1\sigma_0\sin\varphi\left(1+\frac{\gamma_1}{\theta_w}\right) + 2\gamma_1 r\sin\varphi\frac{\partial\sigma_0}{\partial r} + \rho g r\theta_w = \rho\left[r u_0\left(\frac{\partial v_1}{\partial r} + \frac{v_1}{r}\right) + \frac{v_1{}^2}{\theta_w}\right] \tag{22}$$

Third, the θ^2 terms in continuity and the r equation of motion yield

$$r\frac{\partial u_2}{\partial r} + u_2 + \frac{3v_3}{\theta_w} = 0 \tag{23}$$

$$r(1-\sin\varphi)\frac{\partial\sigma_2}{\partial r} - 2\sigma_2\sin\varphi\left(1+\frac{3\gamma_1}{\theta_w}\right) + 4\gamma_1{}^2\sigma_0\sin\varphi\left(1+\frac{\gamma_1}{\theta_w}\right) - 6\frac{\gamma_3}{\theta_w}\sigma_0\sin\varphi + 2r\gamma_1{}^2\sin\varphi\frac{\partial\sigma_0}{\partial r} + 4r\sigma_0\gamma_1\sin\varphi\frac{\partial\gamma_1}{\partial r} + \rho g r\frac{\theta_w{}^2}{2} = \rho\left[r\frac{\partial(u_0u_2)}{\partial r} - \frac{2u_2v_1}{\theta_w} + \frac{v_1{}^2}{r^2}\right] \tag{24}$$

The boundary conditions on the solid side walls are that the normal

velocity v is zero and that γ takes the value of γ_w calculated from the relation (14). Hence

$$0 = v_1 + v_3 + \ldots \tag{25}$$

$$\gamma_w = \gamma_1 + \gamma_3 + \ldots \tag{26}$$

Clearly, the solution is only valid provided each coefficient is much smaller than its predecessor; the conditions on θ_w and γ_w which this implies will be determined as we proceed.

First consider the solution which results when the series for v and γ are both terminated with a single term; it follows from the boundary conditions (25) and (26) that

$$v_1 = 0; \qquad \gamma_1 = \gamma_w. \tag{27}$$

Integration of the forms of equations (19) and (20) which result leads to

$$u_0 = U\left(\frac{r_1}{r}\right) \tag{28}$$

$$\frac{\sigma_0}{\rho g r_1} = \frac{1}{(\omega-1)(1-\sin\varphi)}\left(\frac{r}{r_1}\right) - \frac{F}{(\omega+2)(1-\sin\varphi)}\left(\frac{r_1}{r}\right)^2 + S\left(\frac{r}{r_1}\right)^{\omega} \tag{29}$$

where r_1 is some chosen typical length, the integration constants U and S remain to be determined, F is a modified Froude number U^2/gr_1 and ω is a known quantity calculated from

$$\omega = \frac{2\sin\varphi}{(1-\sin\varphi)}\left(1+\frac{\gamma_w}{\theta_w}\right). \tag{30}$$

It might be noted in passing that though the solution (29) has been obtained for the case in which the wall friction angle, δ, is constant along the walls it is also possible to construct a more general solution in which δ and hence γ_w is some prescribed function of r (Pearce [14]).

Having obtained $u_0(r)$ and $\sigma_0(r)$ except for the two undetermined constants U and S expressions for u_2 and σ_2 then follow simply from (21) and (22):

$$u_2 = -2\theta_w\gamma_w U\left(\frac{r_1}{r}\right) \tag{31}$$

$$\frac{\sigma_2}{\rho g r_1} = \left[\frac{\gamma_w(3\theta_w+2\gamma_w)\sin\varphi}{(\omega-1)(1-\sin^2\varphi)} + \frac{{\theta_w}^2}{2(1+\sin\varphi)}\right]\left(\frac{r}{r_1}\right) - \frac{2{\gamma_w}^2 F\sin\varphi}{(\omega+2)(1-\sin^2\varphi)}\left(\frac{r_1}{r}\right)^2 + \frac{S\gamma_w(\omega\theta_w+2\gamma_w+2\theta_w)\sin\varphi}{(1+\sin\varphi)}\left(\frac{r}{r_1}\right)^{\omega}. \tag{32}$$

Each of the basic equations have thus been used once to produce a solution in which all terms of order θ^3 or greater have been dropped from the expansions (15)–(18). It is particularly significant to note from the results (31) and (32) that the order of magnitude of u_2 is less than that of u_0 by the factor $\theta_w\gamma_w$ and that the order of σ_2 is less than that of σ_0 by the factors $\theta_w\gamma_w$, ${\gamma_w}^2$, and ${\theta_w}^2$. Thus in so far as successive terms have been determined the expansions converge provided θ_w and γ_w are substantially less than unity.

5 Boundary Conditions on the Upper and Lower Surfaces

Before the solution comprised of (27)–(29), (31), and (32) can be used to compute quantities such as net flow rate the constants S and U must be determined by the application of boundary conditions at the upper and lower surfaces. Of these two boundaries it will be seen that provided the approximate positions (Fig. 1) given by $r = r_2$ and r_1, respectively, are such that $r_2/r_1 \ll 1$ then it is particularly important to apply realistic boundary conditions at the discharge from the hopper. Physically what happens at this boundary is that along some line, Γ, such as that dashed in Fig. 2, the intergrain pressure becomes zero ($\sigma = 0$) and below this line the grains effectively freefall with contact which is intermittent at most. Thus the most appropriate condition is that $\sigma = 0$ on some undetermined surface Γ which, in general, does *not* lie on the cylindrical surface $r = r_1$. Since the boundary condition on the upper surface which is located in the vicinity of $r = r_2$ is less critical we shall assume a similar boundary condition for the upper surface even though a number of alternative conditions dependent on the actual hopper problem are possible.

But prior to the application of these conditions it is instructive to simply assume that the surfaces $r = r_1, r_2$ are free surfaces with $\sigma = 0$ and to the first order, to apply $\sigma_0(r_1) = \sigma_0(r_2) = 0$ to the relation (29). Then both S and F (or U) are determined and

$$F = \frac{U^2}{gr_1} = \frac{(\omega+2)}{(\omega-1)}\frac{\left[1-\left(\frac{r_1}{r_2}\right)^{\omega-1}\right]}{\left[1-\left(\frac{r_1}{r_2}\right)^{\omega+2}\right]}. \tag{33}$$

The fact that $\sigma_2(r_1) = \sigma_2(r_2) = 0$ cannot simultaneously be satisfied is simply a reflection of the unjustified assumption that the free surfaces lie on $r = r_1, r_2$. Nevertheless (33) may be regarded as the first-order solution for which the corresponding average discharge velocity $U_D = U$. Note that the character of the solution (33) when $r_2 \gg r_1$ differs according to whether ω is greater or less than unity. This critical value can be seen from the relation (30) to correspond effectively to an internal friction angle greater or less than about 20°, or more precisely

$$\varphi_{\text{critical}} = \sin^{-1}\left[\{3 + 2\gamma_w/\theta_w\}^{-1}\right]. \tag{34}$$

If γ is greater than this then the flow rate given by the result (33) becomes independent of the head or position of boundary $r = r_2$ provided $r_2 \gg r_1$. (In this situation the constant S becomes negligible and the constant F and hence the flow rate is effectively determined by the boundary condition at discharge alone).

To obtain a more accurate result than (33) which includes the $O(\theta_w\gamma_w, {\theta_w}^2)$ terms we assume that the radial distance, $\epsilon(\theta)$, between actual discharge free surface, Γ, and the surface $r = r_1$ (Fig. 2) is given by

$$\epsilon(\theta) = \epsilon_1\left[1-\left(\frac{\theta}{\theta_w}\right)^2\right]. \tag{35}$$

Then the condition that $\sigma = 0$ on this surface is expanded in a Taylor series to obtain the condition

$$\sigma_{r=r_1} + \epsilon_1\left(1-\left(\frac{\theta}{\theta_w}\right)^2\right)\left(\frac{\partial\sigma}{\partial r}\right)_{r=r_1} = 0. \tag{36}$$

Substituting the series expansion (18) this condition yields

$$(\sigma_0)_{r=r_1} + \epsilon_1\left(\frac{\partial\sigma_0}{\partial r}\right)_{r=r_1} = 0 \tag{37}$$

$$(\sigma_2)_{r=r_1} + \epsilon_1\left(\frac{\partial\sigma_2}{\partial r}\right)_{r=r_1} - \epsilon_1\left(\frac{\partial\sigma_0}{\partial r}\right)_{r=r_1} = 0 \tag{38}$$

from which it is clear that ϵ_1 is of order $\theta_w\gamma_w$, ${\theta_w}^2$ and that to this order

$$(\sigma_0 + \sigma_2)_{r=r_1} = 0 \tag{39}$$

$$\epsilon_1 = \frac{(\sigma_2)_{r=r_1}}{(\partial\sigma_0/\partial r)_{r=r_1}}. \tag{40}$$

Using the modified condition (39) at both r_1 and r_2 the corrected result which differs from (33) by factors involving $\theta_w\gamma_w$ and ${\theta_w}^2$ can be written as

$$\frac{U^2}{gr_1} = F = \frac{(\omega+2)}{(\omega-1)}\frac{\left[1-\left(\frac{r_1}{r_2}\right)^{\omega-1}\right]}{\left[1-\left(\frac{r_1}{r_2}\right)^{\omega+1}\right]} \times\left[1+\frac{\theta_w}{2(1+\sin\varphi)}(8\gamma_w\sin\varphi + 3\theta_w\sin\varphi - \theta_w)\right]. \tag{41}$$

Table 1 Some measured properties of granular media

MATERIAL	Mean particle diameter (mm)	Standard deviation (mm)	Particle Specific Gravity	Critical Void Ratio	Bulk Specific Gravity	Internal Friction Angle φ(deg.)*	Surface Friction Angle(δ) with lucite*	Surface Friction Angle(δ) with Aluminum*
Glassbeads:								
P-0140	0.272	0.046	2.47	0.65	1.50	18.2	15.7	
P-0170	0.325	0.041	2.47	0.69	1.46	24.6	15.3	17.7
P-0280	0.592	0.056	2.47	0.67	1.48	24.3	14.4	15.1
V-070	1.326	0.114	2.92	0.71	1.71	26.8	14.2	15.1
V-160	3.23	0.175	2.92	0.76	1.66	31.7	12.9	
Mustard Seed	2.07	0.196	1.22	0.72	0.71	38.2	12.0	
Fine Grain Quartz Sand	0.224	0.074	2.67	0.71	1.56	24.1	20.2	
Medium Grain Quartz Sand	0.317	0.071	2.67	0.75	1.53	30.7	17.9	
Coarse Grain Quartz Sand	0.681	0.109	2.67	0.75	1.53	30.6	14.4	24.5

*Data scatter is less than $\pm 2^\circ$.

Furthermore by including u_2 as given by equation (31), the average discharge velocity, U_D, is simply related to U by

$$U_D = \left(1 - \frac{2}{3}\theta_w\gamma_w\right) U. \tag{42}$$

Combining (41) and (42) one obtains the result

$$\frac{U_D^2}{gr_1} = \frac{(\omega+2)\left[1 - \left(\frac{r_1}{r_2}\right)^{\omega-1}\right]}{(\omega-1)\left[1 - \left(\frac{r_1}{r_2}\right)^{\omega+2}\right]} \times \left[1 + \frac{\theta_w\gamma_w(16\sin\varphi - 8) + \theta_w^2(9\sin\varphi - 3)}{12(1+\sin\varphi)}\right] \tag{43}$$

which is accurate to order $\theta_w\gamma_w$ and θ_w^2. Note that provided φ is greater than 30° the net correction is always positive unlike that indicated by (42) alone. It is convenient to use the hopper opening width, d (Fig. 2), rather than r_1 to define a nondimensional discharge flow rate $U_D/(gd)^{1/2} = U_D/(2gr_1\sin\theta_w)^{1/2}$. It also follows that the maximum separation of the discharge free surface and the cylindrical surface $r = r_1$ is

$$\frac{\epsilon_1}{d} = \frac{2}{3}\frac{\gamma_w\sin\varphi}{(1+\sin\varphi)} + \frac{\theta_w}{12}\frac{(3\sin\varphi - 1)}{(1+\sin\varphi)}. \tag{44}$$

6 Higher-Order Solution

In the preceding section we obtained a solution up to $O(\theta^3)$ in the expansions and that solution indicates that the expansions converge provided $\theta_w \ll 1$, $\gamma_w \ll 1$; we shall see that the solution yields significant improvement in the comparison of theory and experiment over the frictionless wall solution of Sullivan [21]. In terms of the small quantities we have seen that u_0, σ_0 are order unity, v_1 is zero, γ_1 is $O(\gamma_w)$, u_2 is $O(\theta_w\gamma_w)$ and σ_2 contains terms of order θ_w^2 and $\theta_w\gamma_w$. Before proceeding to utilizing the results of that solution, we should briefly examine the nature of the solution to the next highest order. Clearly, this requires that a further term in each of the expansions be included and evaluated. Thus the boundary conditions (25) and (26) on the walls become

$$v_1(r) + v_3(r) = 0; \qquad \gamma_1(r) + \gamma_3(r) = \gamma_w.$$

From equations (19), (21), and (23) it follows that u_0 and γ_3 are now related by the differential equation

$$u_0 = \frac{Ur_1}{r} - \frac{2}{3}\theta_w\gamma_w r\frac{\partial u_0}{\partial r} + \frac{2}{3}\theta_w\gamma_3 r\frac{\partial u_0}{\partial r} + \frac{\theta_w^2}{6}\left\{\frac{\partial}{\partial r}(ru_0) - r\frac{\partial^2(ru_0)}{\partial r^2}\right\} \tag{45}$$

where U is again an arbitrary constant and the last terms involving γ_3 and θ_w^2 represent corrections to the preceding solution. Also

$$v_1 = -v_3 = -\theta_w\frac{\partial}{\partial r}(ru_0). \tag{46}$$

Now γ_3 follows directly from equation (24) and can be evaluated up to and including terms of order θ_w^3, $\theta_w^2\gamma_w$, $\theta_w\gamma_w^2$, and γ_w^3 in the small quantities using the preceding expression (29) for σ_0. Then improved expressions for u_0 and σ_0 accurate up to quartic terms like θ_w^4, $\theta_w^3\gamma_w$, $\theta_w^2\gamma_w^2$, $\theta_w\gamma_w^3$, and γ_w^4 follow from (45) and (20). Consequently, expressions for u_2, σ_2, v_1, v_3, u_4, σ_4 accurate to the same order follow. The algebra is extremely tedious due to the presence of a denominator like the right-hand side of equation (29) caused by the present of σ_0 in the γ_3 term of equation (24) and the details will not be included here. The form of the solution is discussed only to demonstrate feasibility and to show that the next correction to v and γ is cubic order in θ_w and γ_w and the next correction to u and σ is of quartic order.

7 Measurements of Material Properties

Prior to comparison of the results of Section 5 with experiment it is necessary to briefly discuss the required material properties, namely, the bulk density ρ in the flowing state, the internal friction angle φ, and the wall friction angle δ.

Both the experiments and theory concern granular media which are in a flowing state. Most granular materials exhibit dilation as they are subject to loading and reach a critical void ratio at the point of yield and initiation of flow. This critical void ratio appears to be independent of the initial packing and changes little with further deformation or with deformation rate (Taylor [22], Scott [18], Jenike [10]). Thus the relevant bulk density ρ required in the analysis is obtained from the particle material density and the critical void ratio or by other standard means which measure directly the mass of a given volume of granular medium in its critical state.

Pearce [14] measured the relevant material properties of nine different granular media and these are listed in Table 1 (for other measurements see, for example, Weidler and Pasley [24], Drucker, et al.

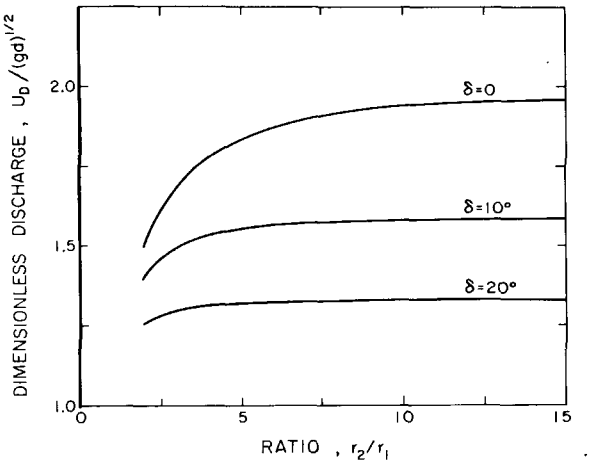

Fig. 3 Variation of dimensionless discharge, $U_D/(gd)^{1/2}$ with hopper height, r_2/r_1, for an opening angle of $\theta_w = 30°$, an internal friction angle of $\varphi = 30°$ and various wall friction angles, δ, as shown

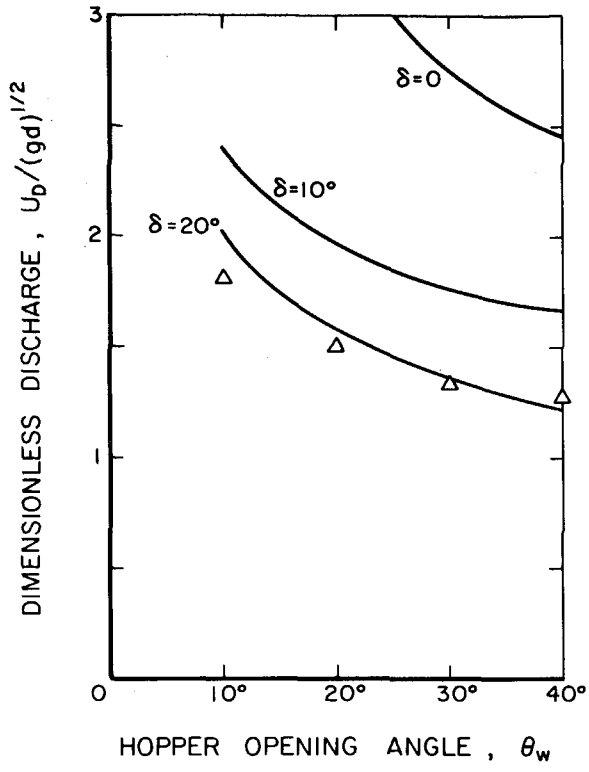

Fig. 4 Asymptotic values of the dimensionless discharge, $U_D/(gd)^{1/2}$, for $r_2/r_1 \gg 1$ and an internal friction angle of $\varphi = 25°$ plotted against the hopper opening angle for various wall friction angles, δ, as shown. The experimental points are measurements of Sullivan [21] on glass beads ($\varphi \approx 25°$) with a wall friction angle δ of 17°.

[6], and Sullivan [21]). The internal friction angles, φ, were measured using a Direct Shear Apparatus (Scott [18]) in which a sample under a given normal load is subjected to shear displacement and the reactive shear force measured. The ratio of the shear force to the normal load reaches a maximum value after sufficient displacement, that value being tan φ where φ is the internal friction angle. For the cohesionless materials tested this angle was virtually independent of the applied normal load and the values are listed in Table 1. The exhibited increase of φ with increasing standard deviation in particle size is worthy of note and may be due to greater interlocking of the grains in the materials with larger variations in particle size. A somewhat similar interlocking phenomena may explain the greater internal friction angle in the more irregular particles such as the sands and mustard seed.

Finally, Pearce also measured surface friction angles between the granular materials of Table 1 and walls made of lucite and aluminum. The device used was similar to that employed for measurement of internal friction but the normal load and shear displacement were applied to lucite and aluminum pads and the inverse tangents of the ratio of shear force to normal loading determined the wall friction angles, δ, listed in Table 1. The scatter in individual friction angle measurements was about ±2°.

8 Comparison With Theory

One of the difficulties in comparing the theoretical results with experiments on the flow through two-dimensional or wedge-shaped hoppers is a frequent lack of data on ρ, φ, or δ. Thus Table 1 and the last section have been included in order not only to report some typical values of these quantities but also to permit comparison with hopper discharge rates measured by Sullivan [21] (the measurements of the last section were performed with granular materials similar to those used by Sullivan).

Sullivan [21] measured discharge flow rates for the P-0170 glass beads and a sand (for which measurements showed $\varphi = 30°$, $\delta = 25°$) through aluminum-plated brass "two-dimensional" hoppers of various opening angles, θ_w. The discharge opening, d, was 6.35 mm (¼ in.) and the flow was bounded in the other dimension by vertical lucite side plates separated by either 55.6 mm or 68.3 mm. This dimensional change had no discernible effect on the results indicating that the frictional effects of these side plates was small. The supply to the hoppers was from a vertical duct 68.3 mm square, the value of r_2/r_1 being 10.75. It was observed that the flow rate was head independent. In Fig. 3 we have plotted the variation of the nondimensional discharge $U_{D0}/\sqrt{gd}$ from equation (43) against r_2/r_1 for a typical opening angle θ_w of 30°, various wall friction angles, δ and a typical internal friction angle, φ, of 30°. It can be seen that provided r_2/r_1 is greater than about 5 the discharge is indeed independent of r_2/r_1 for typical friction angles. The asymptotic values of discharge rate from equation (43) are plotted against θ_w in Figs. 4 and 5 values of φ of 25° and 30° and various wall friction angles. The zero wall friction curves correspond to but are different from those of Savage's [16] frictionless wall theory. Sullivan's [21] experimental data for glass beads ($\varphi \cong 25°$, $\delta \cong 17°$) and for a sand ($\varphi \cong 30°$, $\delta \cong 25°$) are also plotted in Figs. 4 and 5. It can be seen that the agreement between theory and experiment is good in both cases.

Apart from the global property of total discharge we can also compare the variation of the local velocity u with position θ (the velocity profile) with the experiments of Bosely, Schofield, and Shook [1] who made photographic measurements of the particle velocities at discharge from a lucite hopper for which $\theta_w = 32.5°$. Their results for a sand with an effective internal friction angle of 35° are plotted as the ratio of local particle velocity to average particle velocity (like U_D) in Fig. 6. Also shown are the predictions of the present solution for wall friction angles of 0°, 10°, and 20°. It can be seen that the experiments agree well with the theoretical prediction for an expected δ of about 15° (see Table 1). Though we have plotted here the ratios of velocities the total mass discharge rates also agree well with the theory.

Another feature of interest in the theory is the distance ϵ_1 between the discharge free surface at $\theta = 0$ and the cylindrical surface $r = r_1$. This is plotted nondimensionally as ϵ_1/d (from equation (44)) in Fig. 7 as a function of θ_w for a typical value of φ (25°), tall hoppers ($r_1/r_1 \gg 1$) and various wall friction angles. Notice that ϵ_1/d is always small and is only slightly dependent on either φ or θ_w; it is primarily determined by the wall friction angle, δ, being given approximately by $\frac{1}{3}\tan\delta$.

Finally, we have also plotted the variation of the theoretical nondimensional pressure, $\sigma/\rho g r_1$, on the walls with position r/r_1 for a hopper opening angle of 25°, a hopper height of $r_2/r_1 = 18$ and an internal friction angle of 35° in Fig. 8. An experimental "line" given by Handley and Perry [7] is also shown and pertains to a hopper of opening angle 25° and a sand of $\varphi = 35°$, $\delta = 20°$. The scatter on these

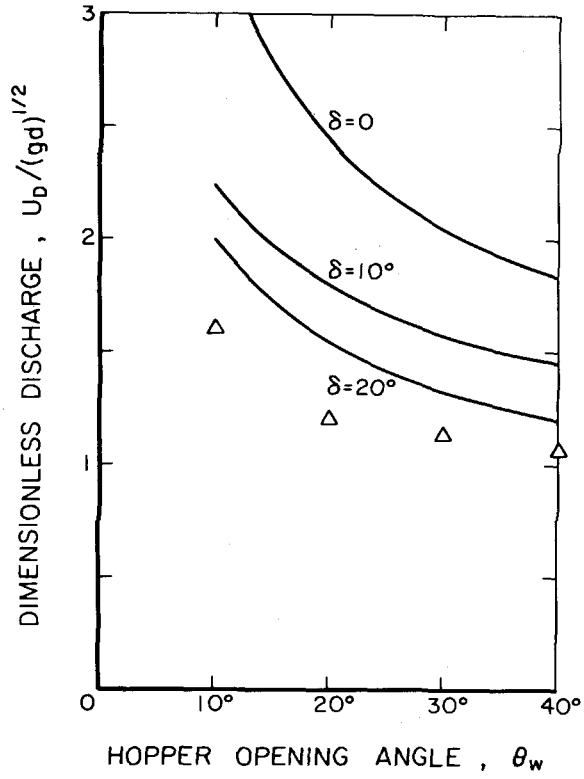

Fig. 5 Asymptotic values of the dimensionless discharge, $U_D/(gd)^{1/2}$, for $r_2/r_1 \gg 1$ and $\varphi = 30°$ plotted against θ_w for various wall friction angles as shown. The experimental points are measurements by Sullivan [21] on a sand for which the measured φ was about 30° and δ was about 25°.

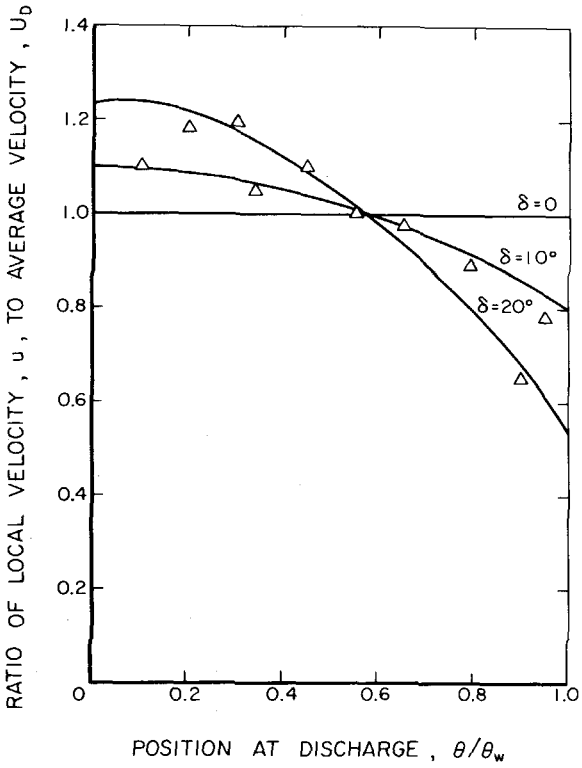

Fig. 6 Ratio of local velocity, u, to average velocity, U_D, at discharge from a $\theta_w = 32.5°$ hopper as function of position, θ/θ_w, for a granular medium with $\varphi = 35°$ and various wall friction angles. Also shown is the experimental data of Bosley, Schofield and Shook [1] for a sand ($\varphi \approx 35°$); the wall friction angle, δ for this data is probably about $15 \Rightarrow 20°$.

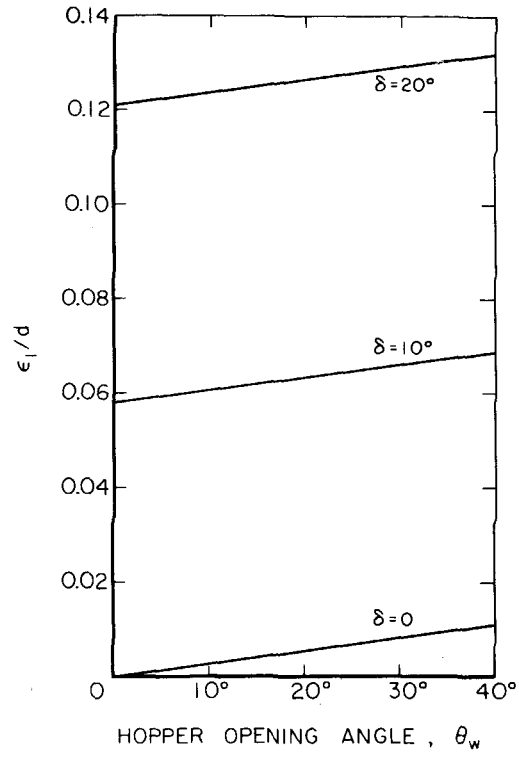

Fig. 7 Position of discharge free surface at $\theta = 0$ plotted against hopper angle, θ_w, for $\varphi = 25°$ and various wall friction angles

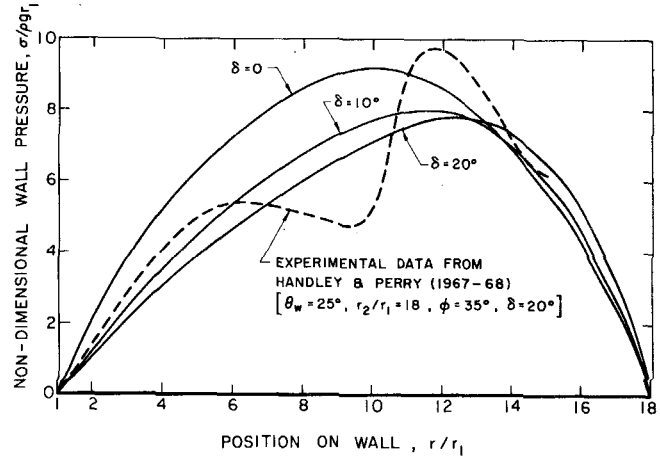

Fig. 8 Nondimensional wall pressure ($\sigma/\rho g r_1$ at the wall) as a function of position, r/r_1, for a 25° hopper for which $r_2/r_1 = 18$, a granular medium of $\varphi = 35°$ and various wall friction angles as indicated. The experimental data given by the dashed line are taken from Handley and Perry [7] for which $\theta_w = 25°$, r_2/r_1, $\varphi \simeq 35°$, and $\delta \simeq 20°$.

experimental measurements was not given by Handley and Perry and hence the experimental line could only be regarded as representative of the trend in these difficult experimental measurements. In this respect the theory would appear to be consistent with the experimental results.

9 Concluding Remarks

We have shown that an analytical solution for the flow of a granular medium in a two-dimensional hopper which is based on the Jenike-Shield constitutive relations yields results which are in good agreement with the experiments as far as hopper discharge and the nature of the flow near discharge are concerned. The solution is restricted to so-called "mass flow hoppers" of moderate opening angle θ_w. The solution demonstrates the well-known experimental fact that the

discharge rate is primarily a function of the conditions at discharge and is independent of the conditions at inlet provided by $r_2/r_1 \gg 1$.

In most experiments on mass flow hoppers the inflow is provided by a vertical duct leading from another supply hopper. Thus there exists a transition from an unyielded plug to the flow in the test hopper; Lee, Cowin and Templeton [12] have observed that this transition can be quite unsteady in some materials. However the flow near discharge appeared to be much more regular and steadier. (In this regard we might mention that an examination of the stability of the present solution to nonsymmetric perturbations indicated that it was always stable under the boundary conditions assumed in Section 5.)

Experiments show that as the angle, θ_w, is increased beyond a certain value the flow in the hopper changes character and takes a form in which flow exists in a central core surrounded by unyielded material. The present solution though restricted to small θ_w does indicate progressively smaller velocities near the walls as θ_w is increased. Indeed the relations (28) and (31) suggest that the wall velocity reaches zero when $\theta_w \approx 2\gamma_w$. Though such angles are beyond the realm of validity of the solution the resulting limiting wall angles in the neighborhood of 50° are not inconsistent with the experimental observations (Wieghardt [25]).

Finally, we should mention that the corresponding solution for conical hoppers should follow lines very similar to those presented here and will be presented shortly.

Acknowledgments

The authors are indebted to Professor R. H. Sabersky for his encouragement and advice in this research. We should also like to acknowledge the support of the National Science Foundation, Union Carbide Corporation, and the Hughes Aircraft Company who supported James C. Pearce with a Doctoral Fellowship during graduate studies at the California Institute of Technology.

References

1 Bosley, J., Schofield, C., and Shook, C. A., "An Experimental Study of Granular Discharge From Model Hoppers," *Trans. Institution of Chemical Engineers*, Vol. 47, 1969, pp. T147-T-152.

2 Drescher, A., and de Josselin de Jong, G., "Photoelastic Verification of a Mechanical Model for the Flow of a Granular Material, *Journal of the Mechanics and Physics of Solids*, Vol. 20, 1975, pp. 337–351.

3 Drescher, A., "An Experimental Investigation of Flow Rules for Granular Materials Using Optically Sensitive Glass Particles," *Geotechnique*, Vol. 26, No. 4, 1976, pp. 591–601.

4 Drucker, D. C., "Limit Analysis of Two and Three-Dimensional Soil Mechanics Problems," *Journal of the Mechanics and Physics of Solids*, Vol. 1, 1953, pp. 217–226.

5 Drucker, D. C., "Coulomb Friction, Plasticity, and Limit Loads," ASME JOURNAL OF APPLIED MECHANICS, Vol. 21, 1954, pp. 71–74.

6 Drucker, D. C., Henkel, D. J., and Gibson, R. E., "Soil Mechanics and Work-Hardening Theories of Plasticity," *Trans. ASCE*, Vol. 122, 1957, pp. 338–346.

7 Handley, M. F., and Perry, M. G., "Stresses in Granular Materials Flowing in Converging Hopper Sections," *Powder Tech.*, Vol. 1, 1967–1968, pp. 245–251.

8 Jenike, A. W., Elsey, P. J., and Woolley, R. H., "Flow Properties of Bulk Solids," University of Utah, Engineering Experimental Station, Bulletin No. 96, Dec. 1958.

9 Jenike, A. W., and Shield, R. T., "On the Plastic Flow of Coulomb Solids Beyond Original Failure," ASME JOURNAL OF APPLIED MECHANICS, Vol. 26, 1959, pp. 599–602.

10 Jenike, A. W., "Steady Gravity Flow of Frictional-Cohesive Solids in Converging Channels," ASME JOURNAL OF APPLIED MECHANICS, Vol. 31, 1964, pp. 5–11.

11 Johanson, J. R., "Stress and Velocity Fields in the Gravity Flow of Bulk Solids, ASME JOURNAL OF APPLIED MECHANICS, Vol. 31, 1964, pp. 499–506.

12 Lee, J., Cowin, S. C., and Templeton, J. S., "An Experimental Study of the Kinematics of Flow Through Hoppers," *Trans. of the Society of Rheology*, Vol. 18, 1974, pp. 247–269.

13 Mandl, G., and Fernandez, L. R., "Fully Developed Plastic Shear Flow of Granular Materials," *Geotechnique*, Vol. 20, No. 3, 1970, pp. 277–307.

14 Pearce, J. C., "Mechanics of Flowing Granular Media," PhD Thesis, California Institute of Technology, Pasadena, California, 1975.

15 Pemberton, C. S., "Flow of Imponderable Granular Materials in Wedge-Shaped Channels," *Journal of the Mechanics and Physics of Solids*, Vol. 13, 1965, pp. 351–360.

16 Savage, S. B., "The Mass Flow of Granular Materials Derived From Coupled Velocity-Stress Fields," *British Journal of Applied Physics*, Vol. 16, 1965, pp. 1885–1888.

17 Savage, S. B., "Gravity Flow of a Cohesionless Bulk Solid in a Converging Conical Channel," *International Journal of Mechanical Sciences*, Vol. 19, 1967, pp. 651–659.

18 Scott, R. F., *Principles of Soil Mechanics*, Addison-Wesley Publishing Company, Inc., 1963.

19 Shield, R. T., "On Coulomb's Law of Failure in Soils," *Journal of the Mechanics and Physics of Solids*, Vol. 4, 1965, pp. 10–16.

20 Sokolovsky, V. V., *Statics of Soil Media*, Butterworth Scientific Publications, 1960.

21 Sullivan, W. N., "Heat Transfer to Flowing Granular Media," PhD Thesis, California Institute of Technology, Pasadena, Calif., 1972.

22 Taylor, D. W., *Fundamentals of Soil Mechanics*, Wiley, New York, 1948.

23 Templeton, J. S., "An Experimental Study of the Mechanics of Rupture Zones in the Gravity Flow of a Granular Material," ASME Applied Mechanics Division publication, *The Effects of Voids on Material Deformation*, Vol. 16, 1976, pp. 71–91.

24 Weidler, J. B., and Pasley, P. R., "Analytical Description of Behavior of Granular Media," *Journal of the Proceedings of the ASCE, Engineering Mechanics Division*, Vol. EM 2, Apr. 1969, pp. 379–394.

25 Wieghardt, K., 1975. "Experiments in Granular Flow," *Annual Review of Fluid Mechanics*, Vol. 7, 1975, pp. 89–114.